(a) Title: Theoretical Methods for the Determination of Mixing

(b) Names and Affiliations of Authors

Baolian Cheng
Applied Physics Division
Los Alamos National Laboratory
Los Alamos, NM 87545

James Glimm
Department of Applied Mathematics and Statistics
Stony Brook University
Stony Brook, NY 11794-3600

and

Center for Data Intensive Computing
Brookhaven National Laboratory
Upton, NY 11973-5000

Hyeonseong Jin
Department of Applied Mathematics and Statistics
Stony Brook University
Stony Brook, NY 11794-3600

David Sharp
Applied Physics Division
and
Theoretical Division
Los Alamos National Laboratory
Los Alamos, NM 87545

(c) Corresponding Author:

James Glimm
Department of Applied Mathematics and Statistics
Stony Brook University
Stony Brook, NY 11794-3600
Email: glimm@ams.sunysb.edu
Phone: (631) 632-8355
Fax: (631) 632-8490

(d) Address for reprints: same as above

(e) Short Title: Theoretical Methods for Mixing

(f) Number of manuscript pages: 19
Number of tables: 1
Number of figures: 5

Abstract:

Theoretical Methods for the Determination of Mixing

Acceleration driven fluid mixing is studied here from a theoretical point of view. Considerable progress has been achieved in the understanding of mix. Theories of the authors are reviewed which allow prediction of the edge of the mixing zone, in agreement with experimental data. Theories which describe the distribution of masses within the mixing region are also reviewed. The theory we present describes a chunk mix regime, in which two phases are mixed at a chunk level, but for which there is no atomic mixing. Thus the two phases are segregated into disjoint regions of space.

Keywords: mixing, multiphase flow, Rayleigh-Taylor instability

1 Introduction

Characterization of mixing rates for acceleration driven flows is important for the design of inertial confinement (ICF) targets and the study of astrophysical flows modeling supernovae and geophysical flows involving thermal inversion or density inversion (e.g. a salt dome) layers. Underprediction of mixing rates from many simulation codes relative to experiments and observational data adds to the importance of a theoretical investigation. Remarkably, the theoretically predicted mixing rates have been in agreement with experiment for some time. In this paper we summarize our main results for the theoretical determination of mixing rates, with an emphasis on recent improvements which add considerably to the power and applicability of these methods. We use these mixing rates to parameterize a subgrid mixing model, also presented here. Detailed analytic solutions to this model have been known for some time. We present the weakly compressible asymptotic expansion (the incompressible limit). We comment on the relation of our results to the direct simulation determination of mixing rates.

The outline of our approach can be summarized as:

1. Bubble merger models to predict bubble growth rate;
2. Characterization of the Center of Mass (COM) motion to link bubble side mix predictions to spike side mix predictions;
3. Determination of drag as a function of Atwood number, so that arbitrary accelerations can be studied;
4. Analytic determination of leading and below leading order large time asymptotics for the edge motion equations;
5. Mix model (subgrid model) equations;
6. Determination of an effective diffusion and Reynolds stress term for use in reduced models.

2 Bubble merger models

Bubble merger models predict the penetration rate of fingers of light fluid (bubbles) into the heavy fluid. For acceleration driven mixing, it is observed that the bubbles increase in size, through a process of bubble competition and merger. In this process, advanced bubbles are accelerated relative to the mean bubble motion, while retarded ones are held back. Thus the smaller bubbles (also generally the retarded ones) become removed from the interface of advancing bubbles, while the larger, advanced ones expand to fill the resulting space. In 1960, Sharp and Wheeler proposed a model to describe this process. The model was corrected by Glimm and Sharp (1990, 1997) to include the hydrodynamical accelerations (positive and negative) given to advanced and retarded bubbles due to their positions relative to the mean bubble penetration height. Such models were extended to three dimensions by Oron et al. (2001) and independently by Cheng et al. (2002a), with improved predictions. The 3D models predict not only the growth rates for the bubble interface (both agree with experiment; Cheng et al. is slightly higher); they also predict the bubble height to width ratio. For this quantity, the two models are distinctly different in their predictions, see Table 1. Agreement of the Cheng et al. model with experimental data is very satisfactory.

[Table 1 goes here]

The bubble dynamic equations are formulated in scaled variables, from which the Agt^2 dynamic growth has been removed. This being the case, the self similar, late time solution appears as a fixed point. In fact, it is a renormalization group (RNG) fixed point.

For steady acceleration, i.e. Rayleigh-Taylor (RT) mixing, the bubble penetration height h_b satisfies the scaling law $h_b = \alpha_b Agt^2$. Four directly measurable quantities determine the growth rate constant α_b in this formula. The measurements, the relation of these quantities to α_b and the experimental validation of this relation are contained in Cheng et al. (2002a). We list the four quantities: (1) Let t'_m be the time to merger for a pair of interacting bubbles. Then $w = \left\langle 1/t'_m \right\rangle_*$ is the mean inverse time to merger, and thus the mean merger rate. It is evaluated at the fixed point. (2) h'_m is the maximum height separation, i.e. the height for instantaneous merger, (3) c_b is the speed of a single bubble in a periodic array, and (4) k is a geometrical factor giving the increase in radius for a single merger event, slightly less than ½Each of the proceeding is expressed in scaled units. Then the fixed point formula for α_b is:

$$\alpha_b = \frac{k}{4}(c_b + \frac{1+k}{2} h'_m w)w \ . \qquad (2.1)$$

As written, the equation has been verified by direct comparison to experimental data, Cheng et al. (2002a). To obtain a closed expression for α_b, the above quantities are evaluated directly within a statistical model for the bubble dynamics. Two quantities define this model: the bubble velocity and the bubble merger criteria. The bubble velocity is defined as the sum of a single (periodic array) bubble velocity and a bubble interaction term, the "envelope velocity". The bubble velocity as a sum of these two terms has been tested against simulation data. The criteria for bubble merger is defined to be the time at which the retarded bubble starts to move backwards, using this two term formula for the bubble velocity. Note that the bubble interaction term can have either sign, so that a zero total velocity is possible. The bubble merger criteria was shown to be an insensitive parameter in the model.

From these two inputs, w and h'_m are determined. The result is the determination $\alpha_b \approx 0.5 - 0.6$, in agreement with experimental results. The same formulas yield the bubble height to width ratio, cited in Table 1. Since (2.1) depends on two parameters, it is important to check it (as we do) on two independent sets of data. Specifically, w is very sensitive to the bubble width while α_b can mask canceling errors between w and h'_m.

3 Compressible mixing zone dynamics

The bubble merger model is readily extended to compressible flow. The single bubble velocity, c_b in scaled variables, must be determined for compressible flow. This quantity affects the envelope velocity and thus the total bubble velocity. The remainder of the analysis is unchanged. See Chen et al. (1993). This same reference shows that a_b increases with increasing values of the dimensionless compressibility $l g / c_h^2$. It was also shown that the bubble merger model predictions for a_b, as corrected in this manner for compressibility, were in good to moderate agreement with simulation results.

4 Center of mass motion

For steady acceleration (Rayleigh-Taylor) incompressible mixing, the center of mass Z_{COM} of the mixing zone satisfies $Z_{COM} = a_{COM} A g t^2$, in accordance with the self similar scaling of the flow. $Z_{COM} \approx 0$ for Atwood numbers $A < 0.8$. For general values of A, the scaling law $a_{COM} = const. A^g$ fits the data. Here the constant is determined by the known value $a_s = 1/2$ for $A = 1$ (free fall) and an assumed value for a_b, while $g \approx 10$ is insensitive to the data. Thus Z_{COM} and a_{COM} very efficiently constrain the self similar flow. The COM relation introduces a new equation which establishes a link between the bubble and spike mixing growth rates. Given a value for a_{COM}, we have determined that the ratio a_s / a_b is a solution of a quadratic equation. Thus spike data can be predicted from a knowledge of bubble data. See Glimm et al. (1999) and Cheng et al. (1999 and 2000). See Fig. 1.

[Figure 1 goes here.]

5 Buoyancy drag equations

A number of authors have considered buoyancy drag equations to describe the dynamics of the edge of the mixing zone. These equations are fundamental for all models of mix, as the data they supply is of such basic importance. Our version of these equations has fewer parameters and greater predictive power than similar equations introduced by others. See Cheng et al. (2000). In addition, we have a finite drag coefficient in the limit $A = 1$, as is required on intuitive grounds. The equations have the form

$$(r_i + k_i r_{i'}) \frac{dV_i}{dt} = (r_i - r_{i'}) g(t) - (-1)^i \frac{C_i r_{i'} V_i^2}{|Z_i|}. \qquad (5.1)$$

Note that the density $r_{i'}$ in the drag term in (5.1) is the density of the fluid being displaced. This form of drag is taken by classical text books in fluid dynamics, but has been incorrectly replaced by r_i, the density of the displacing fluid, by a number of workers, leading to a divergent drag coefficient in the limit $A \to 1$.

Here $k_i = 1$ is an added mass coefficient, Z_i is the penetration distance of the mixing zone on side $i = 1$ (bubble) and $i = 2$ (spike), V_i is the edge velocity and C_i is the drag coefficient. Also $g(t)$ is the acceleration.

There is only one undetermined parameter in (5.1), namely C_1 (as C_2 is determined from C_1 by the COM theory). C_i itself is determined from our bubble merger model, or simulations, or from experiment. Substituting the $h_i = \alpha_i A g t^2$ late time asymptotic solution for RT mixing, we can determine α_i uniquely in terms of C_i and conversely. Thus the equation is completely determined by the RT data, and in view of Sec. 4, it is uniquely determined in terms of the RT bubble data alone (with exceptions noted above for large A).

Thus (5.1) can be used to predict Richtmyer-Meshkov (RM) mixing rate exponents q_i. The late time RM asymptotics are predicted for the first time from the α_i and usually from α_b alone We obtain a zero parameter agreement with experiment and with known $A = 1$ spike limits. See Cheng et al. (2000). See Fig. 2.

[Figure 2 goes here]

For $g(t) = g$ a constant (steady RT mixing), the large time asymptotic solution of the buoyancy drag equation (5.1) is $|Z_i| = \alpha_i A g t^2$. The equation cannot be integrated in closed form for general t, but a closed form approximate evaluation of the next two lower orders (the term proportional to t and the constant term) was obtained. The result exhibited an explicit dependence of these lower order terms on the initial conditions, in contrast to the leading order asymptotics, which is independent of initial conditions. The result is

$$|Z_i(t)| = \alpha_i A g (t - t_0)^2 + b_i \sqrt{\alpha_i A g |Z_{i0}|}(t - t_0) + g_i |Z_{i0}|, \tag{5.2}$$

where Z_{i0} is an initial amplitude, and V_{i0} is an initial velocity. We also define $\alpha_i = 1/(2\sqrt{\alpha_i})$ and $f_{i0} = (1 - \alpha_i |V'_{i0}|)/(1 + \alpha_i |V'_{i0}|)$ as a transform of the scaled initial velocity $V'_i = V_i / \sqrt{Ag|Z_i|}$. Then with

$$d_i = \frac{2(1 + f_{i0}) - \alpha_i (1 + 3 f_{i0})}{(1 + f_{i0})(1 - \alpha_i)} \tag{5.3}$$

a computation shows that $b_i = 2d_i$ and $g_i = d_i^2$. Note the explicit dependence on initial conditions in the lower than leading order terms.

This analysis allows an improved fit and interpretation of experimental data. For example the data of Smeeton and Youngs and of Read can be reliably

distinguished from the leading order asymptotics and the dependence of this data on $Z(t=0)$ or $V(t=0)$ can be observed. See Fig. 3.

[Figure 3 goes here]

Speculations concerning the cause of discrepancy between simulation and experiment have focused on three possible explanations: (a) numerical diffusion in the untracked simulations, (b) preasymptotic behavior in the simulations, and (c) noise in the experiments of a specific spectral power that generates t^2 modification to the t^2 experimental data. Issue (a) is in fact a sufficient explanation, see George et al. (2002). It is possible that (b) may be a contributing explanation. To explore this possibility, the preasymptotic solutions (5.2) of (5.1) will be helpful. Issue (c) is discussed in Glimm et al. (2001).

6 Mix model equations

Two phase flow equations appropriate to a chunk mix regime have been proposed and studied in detail, see Glimm et al (1998 and 1999) and related papers. The model has several attractive features: it is mathematically stable, i.e. totally hyperbolic with real characteristics for time propagation. The equations are thermodynamically determinate, using equation of state models for each constituent in an unmixed mode. Commonly used mix models fail one or both of these properties. In fact a thermodynamically determinate set of equations is often achieved by assumption of molecular mix, leading to models which possess a single temperature.

The chunk mix equations have been analyzed in great detail, with closed form solutions obtained for the incompressible limit, Glimm et al (1998 and 1999). Perturbation terms in the weakly compressible limit have been computed in closed form through second order in the Mach number, Jin (2001) and Glimm & Jin (2001). This is the order for which the incompressible pressure first appears. Results for the volume fraction in this limit are displayed in Fig. 4.

[Figure 4 goes here]

Here we discuss new insight regarding closure which has emerged from a study of the weakly compressible theory. The equations resemble the Euler equations for each fluid considered separately. They are coupled through three interface terms. Two of these are a term $p^* \partial b_k / \partial z$ added to the momentum equation for species k and a term $(pv)^* \partial b_k / \partial z$ is added to the energy equation, also for species k. Here b_k is the volume fraction of species k. We use the notation X^* to denote the quantity X averaged over the interface, and X_k to denote a volume average of X over the phase volume occupied by species k. Closure assumptions, such as neglect of Reynolds stress terms within a single species phase average, and an assumed identity of volume and mass weighted averages within a single phase

average are discussed in Glimm et al. (1998) and earlier papers. The third interface term occurs in the (new) interface equation

$$\frac{\partial b_k}{\partial t} + v^* \frac{\partial b_k}{\partial z} = 0 . \tag{6.1}$$

. The important closure relations are those for the interface quantities p^* and $(pv)^*$ and v^*. The closure for $(pv)^*$ is highly constrained in terms of the v^* and p^* closures. These two are also constrained to be convex combinations of the corresponding phase quantities, v_k and p_k, with convex coefficients $m^x_{k'}$, $x = v, p$. We make the hypotheses (appropriate for a chunk mix regime) that there are no internal length scales within the mixing layer, so that the $m's$ must be functions of dimensionless variables, such as b_k. Taking the functional dependence to be fractional linear in b_k, all but one of the four parameters in the fractional linear dependence is determined in an obvious manner by the boundary conditions at $z = Z_k$, the edges of the mixing zone. In this way the closure is mainly driven by directly observable data, a feature which the authors regard as highly desirable. In fact the edges Z_k are determined by the buoyancy equation (5.1). The closure relation for p^* is set in terms of the ratio of densities Glimm et al. (1998) and Glimm & Jin (2001). We now discuss the v^* closure relation, i.e. the equation for the fractional linear definition of m^v_k in

$$v^* = m^v_2 v_1 + m^v_1 v_2 . \tag{6.2}$$

After inserting obvious mixing zone boundary constraints, and our assumed form m^v_k, we have

$$m^x_k = \frac{b_k}{b_k + c^x_k(t) b_{k'}}, \quad x = v, p . \tag{6.3}$$

. c^v_k was interpreted as a ratio of the volumetric growth rates for the mixing zone for the two phases, $c^v_k = | V_{k'} / V_k |$, in the incompressible case, Glimm et al. (1998 and 1999). Here $V_k = \partial Z_k / \partial t$. As is observed below, both the convex sum property (6.2) and the fractional linear form (6.3) for the convex coefficients can be derived from the primitive equations, and are thus independent of closure assumptions. Closure thus is a specification of c^v_k.

The volumetric mixing rate constraint determining the v^* closure has been extended to the fully compressible case Glimm & Jin (2001). Because of compressibility, new terms enter into the phase volume growth rates, including the compressibility of the two phases. In dimensionless terms, this influence enters as a ratio of the sound speeds for the two fluids in the weakly compressible limit. We start with an exact identity for c^v_k, valid for the fully compressible two fluid equations, derived in the absence of any closure assumptions at all. Note that

the interface equation, the convex sum property for v^* and the fractional linear form for m_k^v are all *derived* in this equation independently of closure assumptions. We have

$$c_k^v = \frac{\frac{\partial v_{k'}}{\partial z} + \frac{1}{r_{k'}} \frac{D_{k'} r_{k'}}{Dt}}{\frac{\partial v_k}{\partial z} + \frac{1}{r_k} \frac{D_k r_k}{Dt}} \tag{6.4}$$

is the ratio of logarithmic rates of volume creation for the two species, where $D_k / Dt = \partial / \partial t + v_k \partial / \partial t$ is the convective derivative defined by the velocity v_k. Then the closure (absence of internal length scales) can be interpreted as an equation for c_k^v, namely

$$\frac{\partial c_k^v}{\partial z} = 0 . \tag{6.5}$$

It is of interest to analyze the v^* closure in the weakly compressible perturbative analysis. There we find that the incompressible pressures, the ratios of the compressible sound speeds, the second order contribution to the phase volume expansion ratio $|V_k / V_{k'}|$, and the second order perturbation term in the expansion of c_k^v are linked by a newly derived equation (Jin (2001), Glimm & Jin (2001)). This equation removes an indeterminancy in the incompressible equations, previously not understood, and shows that the two phase incompressible equations, in contrast to the single phase case, remember the compressible fluids from which they are derived. We first reformulate (6.5) as

$$c_k^v = \frac{\int_{Z_k}^{Z_{k'}} \left(\frac{\partial v_{k'}}{\partial z} + \frac{1}{r_{k'}} \frac{D_{k'} r_{k'}}{Dt} \right) dz}{\int_{Z_k}^{Z_{k'}} \left(\frac{\partial v_k}{\partial z} + \frac{1}{r_k} \frac{D_k r_k}{Dt} \right) dz} . \tag{6.6}$$

The formula (6.6) can now be expanded perturbatively in powers of the Mach number, and the second order term in this expansion includes the incompressible pressure. The resulting equation is the desired new equation for the incompressible pressure. See Jin (2001) and Glimm & Jin (2001).

On the basis of the above analysis, we are able to link the phenomenological drag coefficients in the buoyancy drag equation for the edge motion with fundamental laws of physics. Newton's law of acceleration, applied at the edge of the mixing zone is equivalent to the momentum equation, evaluated at this location. The equations can be highly simplified in this evaluation (Glimm et al. (1999)) and resemble buoyancy drag equations (5.1). In fact, they are different, due to the absence of phenomenological quantities. Thus the added mass and the drag are replaced by exact quantities, which, however, are not convenient to evaluate. Specifically they relate to the pressure difference between the phases and the

gradient of the pressure difference. A closed form solution for the pressure equation in the incompressible limit, to be published, reveals terms which can be readily identified as inertial terms (added mass), fundamentally exact drag terms (depending on velocity differences) and pressure difference terms (interpreted as phenomenological corrections to the drag terms). Thus we see that the buoyancy drag equations can be obtained via a closure relation which expresses the added mass and drag as pressure difference terms in the exact momentum equation and relates these to quantities known in the buoyancy drag equation, namely lengths, velocities and accelerations.

7 Effective diffusion and Reynolds stress

Reduced multiphase mixture models have fewer equations and fewer variables. They are logically derived from more complete models. Here we derive a single velocity, single temperature model from the chunk mix model of Sect. 6, following Cheng et al. (2002b). For models with a single velocity, this velocity will express mean fluid flow, and cannot drive the mixture process, which is then modeled as a diffusion process. The point is to determine the (time and spatially dependent) interspecies diffusivity, which governs the mixing rates diffusivity. Assuming this to be a function of the volume fraction b_k, Alon & Shvarts (1996) propose diffusion proportional to $b_k(1-b_k) = b_1 b_2$. We find corrections to this form which reflect the deviation of the volume fraction from being a linear function of z.

The key to the computation of the diffusivity is a determination of entrainment time. For a given parcel of fluid k at a given space time location within the mixing zone, the entrainment time is defined to be (the earlier) time at which that parcel entered the mixing zone. Given the velocity history of the two phases, available in closed form (in terms of the edge positions Z_k), one integrates backward in time until the moving edge $Z_{k'}(s)$ is encountered. This motion is then interpreted as a diffusion process, and the exact value of diffusion which duplicates this motion is determined. For RT mixing, the diffusivity can be determined in closed form, while for RM mixing, the diffusivity is solved via an approximate closed form expression, and also by integration of an ordinary differential equation. For the general case, the solution is given up to a quadrature. For the RT case the closed form expression for the diffusivity D is

$$D = 2A^2 g^2 t^3 b_1 b_2 a_1^2 a_2^2 \left[\frac{b_1^2 a_1}{a^3} + \frac{b_2^2 a_2}{a^3} \right]$$

where

$$a = a_1 b_1 + a_2 b_2 .$$

Note that the formula is not symmetric between b_1 and b_2 since $a_1 \neq a_2$ for $A > 0$. The factor in the square brackets is the correction to the formula of Alon & Shvartz (1996). This factor reflects the lack of symmetry between the two phases and is especially significant for Richtmyer-Meshkov mixing. See Fig. 5.

The dominant component R_{zz} of the Reynolds stress tensor is also determined in Cheng et al. (2002b).

[Figure 5 goes here]

8 Conclusions

Theory has been shown to be remarkably successful for the study of turbulent mix. Zero parameter models of the compressible mixing zone have been derived from totally theoretical considerations, and match experiment quantitatively. Both mixing zone edges and the mixing zone interior flow variables have been modeled. The latter are described by a new set of averaged equations, with several pleasant properties, including stability at a hyperbolic level of time propagation, and multi species thermodynamics. Simpler models, such as turbulent diffusive mixing have been derived from these equations. Details of the weakly compressible limit for our averaged equations have been solved in closed form.

9 References

Alon, U. & Shvarts, D. (1996). In *Proceedings of the Fifth International Workshop for Compressible Turbulent Mixing*, pp.14-22. Singapore: World Scientific.

Chen, Y., Deng, Y., Glimm, J., Li, G., Sharp, D.H. & Zhang, Q. (1993). *Phys. Fluids A.* **5,** 2929-2937.

Cheng, B., Glimm, J., Saltz, D. & Sharp, D.H. (1999). *Physica D.* **133,** 84-105.

Cheng, B., Glimm, J. & Sharp, D.H. (2000). *Phys. Lett. A.* **268,** 366-374.

Cheng, B., Glimm, J. & Sharp, D.H. (2002a). *Chaos,* **12**, 267-274.

Cheng, B., Glimm, J. & Sharp, D.H. (2002b). *Zeitschrift fur Angewandte Mathematik und Physik*. 53, 211-238.

Dimonte, G. (2000). *Phys. Fluids.* **7,** 2255-2269.

Dimonte, G. & Schneider, M. (1996). *Phys. Rev. E.* **54,** 3740-3743.

George, E. Glimm, J., Li, X.L., Marchese, A. & Xu, Z.L. (2002). *Proceedings National Academy of Sciences*. **99**, 2587-2592.

Glimm, J., Grove, J., Li, X., Oh, W. & Sharp, D.H. (2001). *J. Comp. Phys.* **169,** 652-677.

Glimm, J. & Jin, H. (2001). *Bol. Soc. Bras. Mat.* **32**, 213-236.

Glimm, J., Saltz, D. & Sharp, D.H. (1998). In: *Nonlinear Partial Differential Equations* Singapore: World Scientific.

Glimm, J., Saltz, D. & Sharp, D.H. (1999). *J. Fluid Mech.* **378,** 119-143.

Glimm, J. & Sharp, D.H. (1990). *Phys. Rev. Lett.* **64,** 2137-2139.

Glimm, J. & Sharp, D.H. (1997). In: *Stochastic Partial Differential Equations: Six Perspectives* Providence: American Mathematical Society.

Jin, H. (2001). Ph.D. Thesis. University at Stony Brook.

Oron, D., Arazi, L., Kartoon, D., Rikanati, A. Alon, A. & Shvarts, D. (2001). *Phys. Plasmas.* **8,** 2883-2889.

Smeeton, V.S. & Youngs, D.L. (1987). Report number 0 35/87. Atomic Weapons Establsihment, Aldermaston, UK.

TABLES

Table 1. Bubble height to width ratios in experiments and models.

Cheng et al. (2002a): Model	3
Oron et al. (2001): Model	1 to 1.5
Smeeton and Youngs (1987): Experiment	3.3
Dimonte and Schneider (1996): Experiment	2 – 4

FIGURE CAPTIONS

Figure 1. The ratio α_s / α_b is determined by a COM assumption and compared to the experimental data of Dimonte et al. (2000) and to a power law fit. The power law is unphysical for $A = 1$, and thus this fit fails to reproduce the experimental data for large A. Our values for α_s / α_b agree with the experimental data for all values of A.

Figure 2. The exponent q_s for RM mixing. The solid and dotted lines are the predictions of Cheng et al. (2000) for $\alpha_b = 0.05$ and for $\alpha_b = 0.06$ respectively. The solid dots are LEM experiments of Dimonte & Schneider (1996).

Figure 3. Dependence of the exact solution of (4.1) on variation of the initial data Z_{b0}. The best fitting value for the data of Smeeton and Youngs (1987) is $Z_{b0} = 0.75$ for their experiment number 101.

Figure 4. Volume fraction of the light fluid, showing the incompressible solution, a perturbation term, and the compressible solution computed perturbatively through first order.

Figure 5. The diffusion coefficient D across the mixing layer in RT mixing. The dash-dotted line is for $A = 0.5$, $\alpha_2 = 0.07$ and the solid line is for $A = 0.96$, $\alpha_2 = 0.18$.

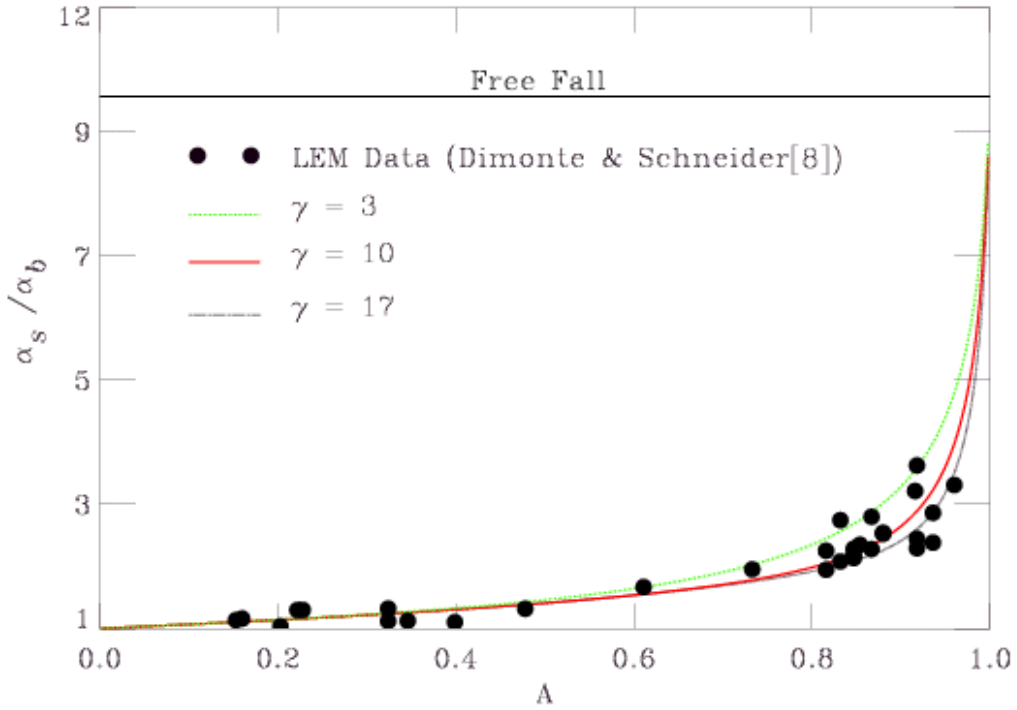
12
9
7
5
3
1
Free Fall
LEM Data (Dimonte & Schneider[8])
γ = 3
γ = 10
γ = 17
α_s / α_b
0.0
0.2
0.4
0.6
0.8
1.0
A

Figure 1

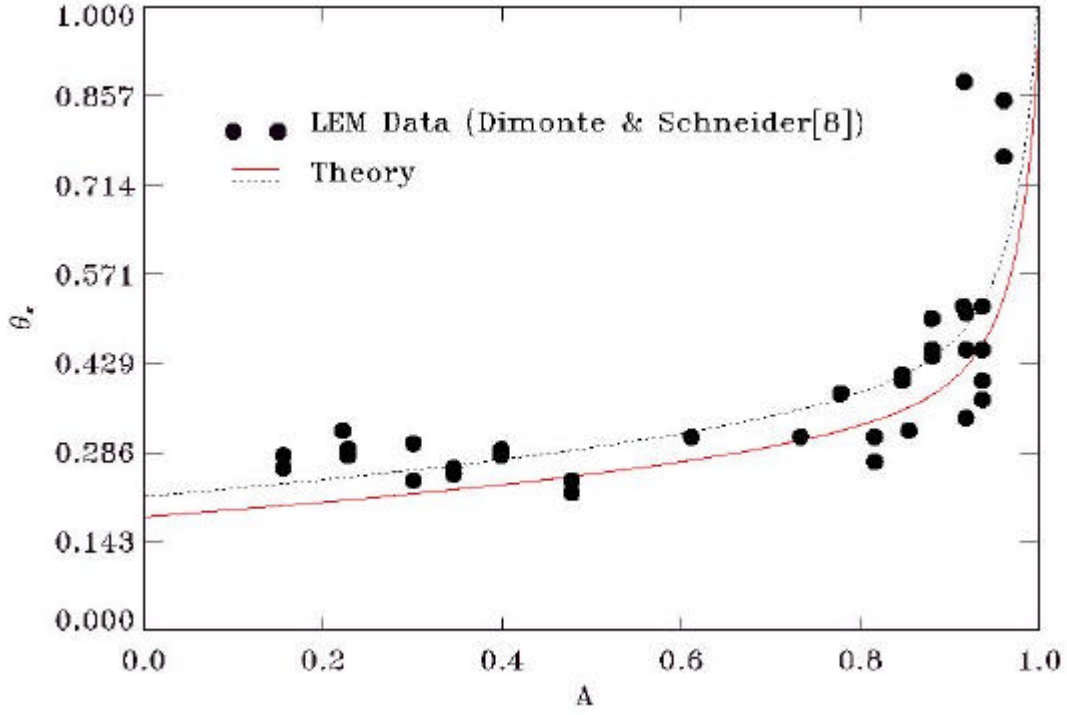
1.000
0.857
0.714
0.571
0.429
0.286
0.143
0.000
θ_r
LEM Data (Dimonte & Schneider[8])
Theory
0.0
0.2
0.4
0.6
0.8
1.0
A

Figure 2

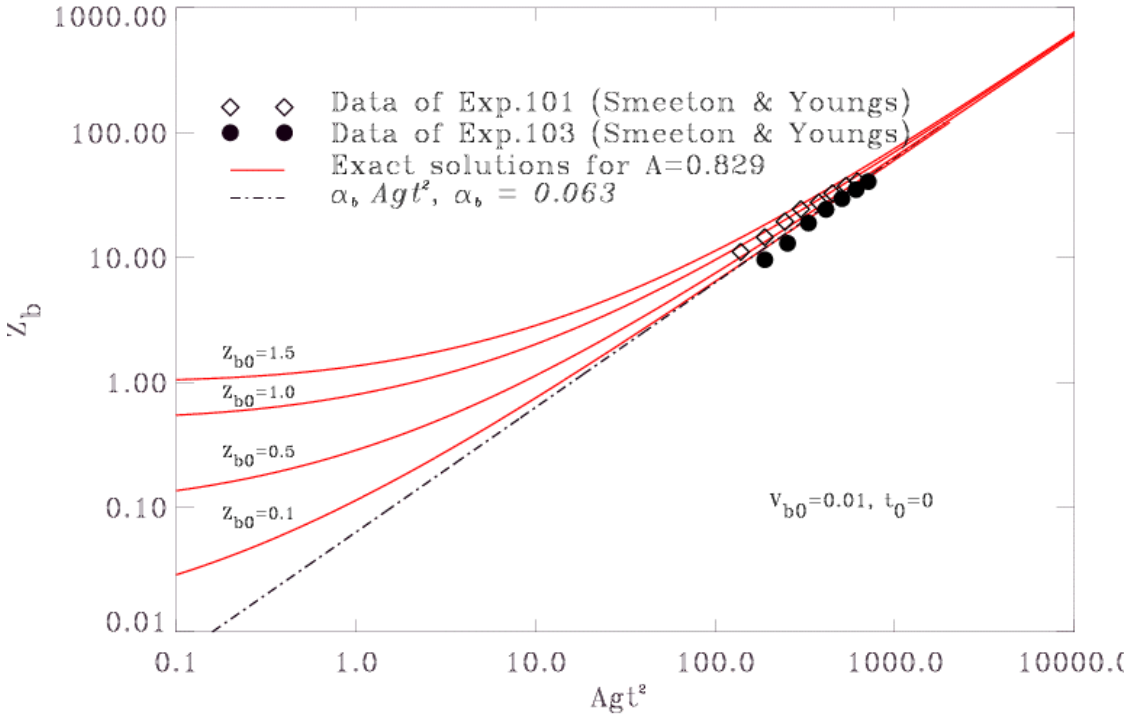
1000.00
100.00
10.00
1.00
0.10
0.01
Z_b
0.1
1.0
10.0
100.0
1000.0
10000.0
Agt^2
Data of Exp.101 (Smeeton & Youngs)
Data of Exp.103 (Smeeton & Youngs)
Exact solutions for A=0.829
$\alpha_b\ Agt^2$, α_b = 0.063
Z_{b0}=1.5
Z_{b0}=1.0
Z_{b0}=0.5
Z_{b0}=0.1
V_{b0}=0.01, t_0=0

Figure 3

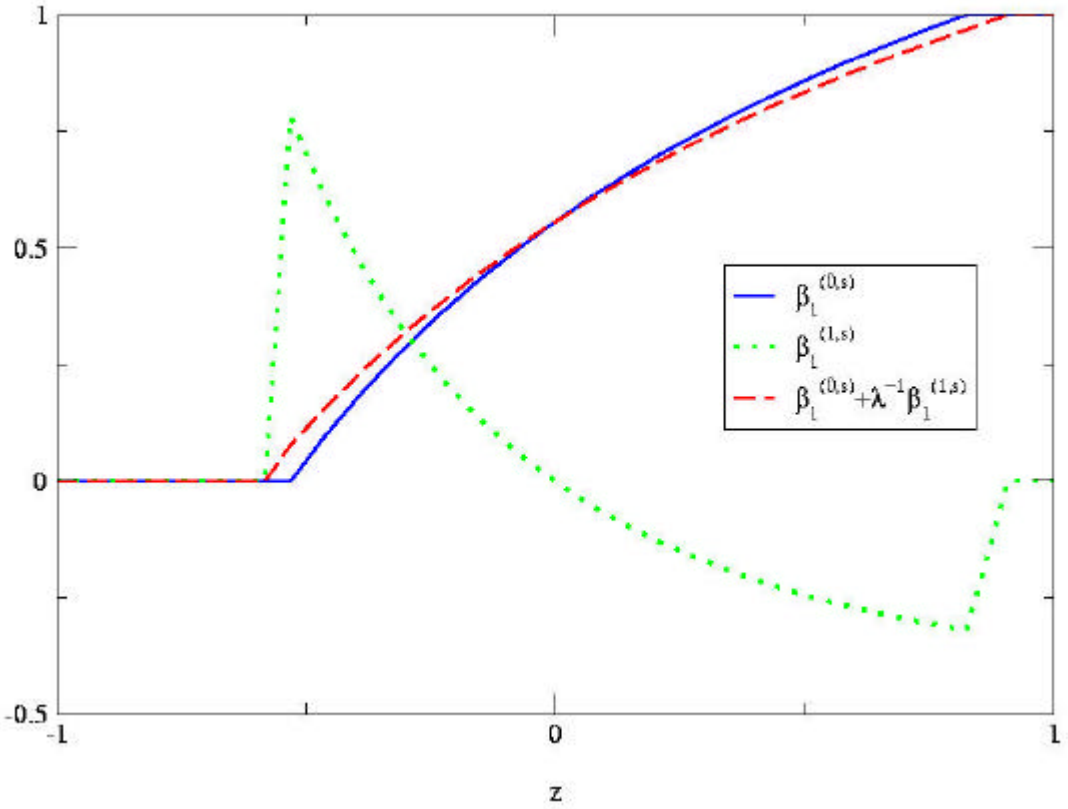

Figure 4

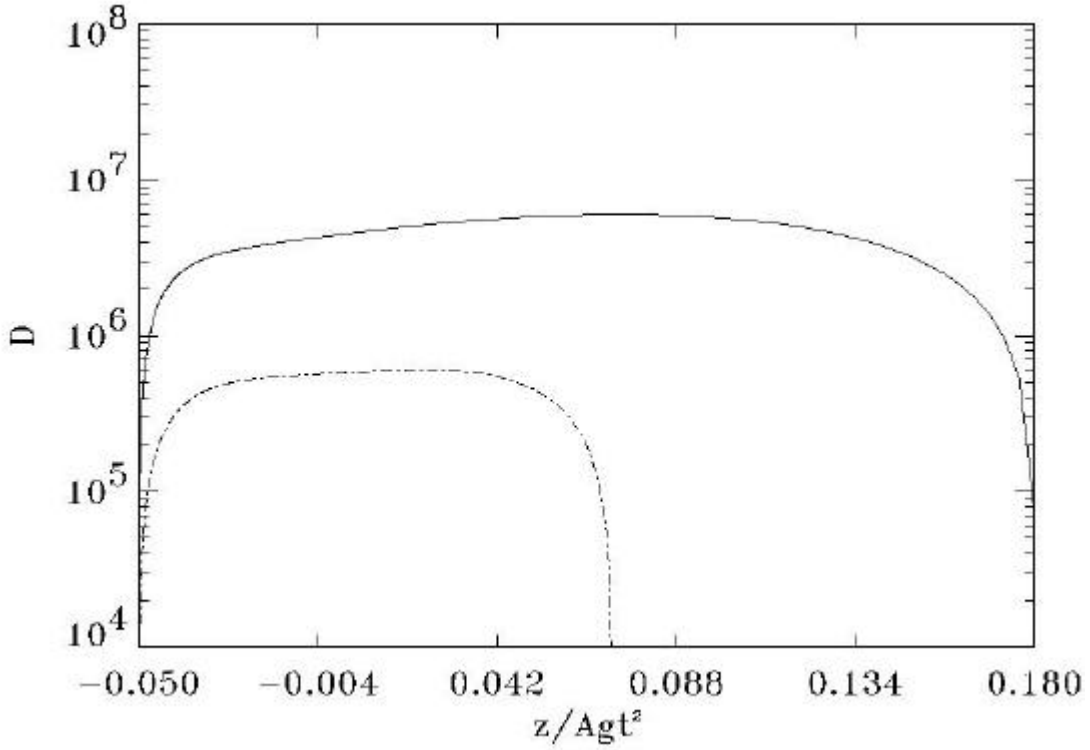

Figure 5